NASA CR-168324
WESTINGHOUSE R&D REPORT 83-9C1-LKOOL-R1
CONTRACT NO. NAS3-22877

MEASUREMENT OF HEAT PUMP PROCESSES INDUCED BY LASER RADIATION

November 1983

WESTINGHOUSE ELECTRIC
R&D Center

1 Report No	2 Government Accession No	3 Recipient's Catalog No
NASA CR-168324		

4 Title and Subtitle	5 Report Date
MEASUREMENT OF HEAT PUMP PROCESSES INDUCED BY LASER RADIATION	November 1983
	6 Performing Organization Code
7 Author(s)	8 Performing Organization Report No
M. Garbuny and T. Henningsen	(W) R&D 83-9C1-LKOOL-R1
	10 Work Unit No
9 Performing Organization Name and Address	
Westinghouse Electric Corporation Research and Development Center Pittsburgh, PA 15235	11 Contract or Grant No NAS3-22877
	13 Type of Report and Period Covered Contractor Report
12 Sponsoring Agency Name and Address	14 Sponsoring Agency Code
National Aeronautics and Space Administration NASA Lewis Research Center 21000 Brookpark Road, Cleveland, OH 44135	

15 Supplementary Notes

16 Abstract

The objective of this work was to demonstrate and measure laser induced cooling predicted, as a result of a theoretical study under a preceding NASA-Ames contract, to be possible in diatomic gases. A series of experiments was performed in which a suitably tuned CO_2 laser, frequency-doubled by a Tl_3AsSe_3 crystal, was brought into resonance with a P-line or two R-lines in the fundamental vibration spectrum of CO. Cooling or heating produced by absorption in CO was measured in a gas-thermometer arrangement. P-line cooling and R-line heating could be demonstrated, measured, and compared. The experiments were next continued with CO mixed with N_2 added in partial pressures from 9 to 200 Torr. It was found that an efficient collisional resonance energy transfer from CO to N_2 existed which increased the cooling effects by one to two orders of magnitude over those in pure CO. Temperature reductions in the order of tens of degrees Kelvin were obtained by a single pulse in the core of the irradiated volume. These measurements followed predicted values rather closely, and it is expected that increase of pulse energies and durations will enhance the heat pump effects. Thus the experiments confirm the feasibility, in principle, of quasi-isentropic engines which convert laser power into work without the need for heat rejection. Of more immediate potential interest is the possibility of remotely powered heat pumps for cryogenic use, and such applications are discussed to the extent possible at the present stage.

17 Key Words (Suggested by Author(s))		18 Distribution Statement
Cooling	Molecular	Unclassified - unlimited
Heating	Gases	
Laser	Diatomic	
Induced	Radiation	
Heat pump	Coherent	

19 Security Classif (of this report)	20 Security Classif (of this page)	21 No of Pages	22 Price*
Unclassified	Unclassified	52	

* For sale by the National Technical Information Service Springfield Virginia 22161

Page intentionally left blank

Page intentionally left blank

ACKNOWLEDGMENTS

B. Sater of NASA-Lewis has been the Technical Monitor of this contract, and the authors wish to express their appreciation for his encouragement and patience. Thanks are also due to K. D. Grimmett who assisted with the experimentation and J. R. Auld for his help with the vacuum and high gas purity system.

Page intentionally left blank

Page intentionally left blank

TABLE OF CONTENTS

LIST OF FIGURES

LIST OF TABLES

Page intentionally left blank

Page intentionally left blank

SUMMARY

The objective of this work was to demonstrate and measure laser induced cooling predicted, as a result of a theoretical study under a preceding NASA-Ames contract, to be possible in diatomic gases. A series of experiments was performed in which a suitably tuned CO_2 laser, frequency-doubled by a Tl_3AsSe_3 crystal, was brought into resonance with a P-line or two R-lines in the fundamental vibration spectrum of CO. Cooling or heating produced by absorption in CO was measured in a gas-thermometer arrangement. P-line cooling and R-line heating could be demonstrated, measured, and compared. The experiments were next continued with CO mixed with N_2 added in partial pressures from 9 to 200 Torr. It was found that an efficient collisional resonance energy transfer from CO to N_2 existed which increased the cooling effects by one to two orders of magnitude over those in pure CO. Temperature reductions in the order of tens of degrees Kelvin were obtained by a single pulse in the core of the irradiated volume. These measurements followed predicted values rather closely, and it is expected that increase of pulse energies and durations will enhance the heat pump effects. Thus the experiments confirm the feasibility, in principle, of quasi-isentropic engines which convert laser power into work without the need for heat rejection. Of more immediate potential interest is the possibility of remotely powered heat pumps for cryogenic use, and such applications are discussed to the extent possible at the present stage.

1. BACKGROUND, MOTIVATION, AND SUMMARY OF RESULTS

The present work has been motivated by the results and predictions of previous studies: first, on the remote operation of thermal laser engines by resonance absorption heating;[1] second, on isentropic engine processes employing both heating and cooling.[2] This second study proposes that, since coherent radiation is free of entropy, it should in principle be possible to remotely power an engine by a laser beam without the need for heat, i.e., entropy, rejection. In its various possible forms of embodiment, the thermodynamic cycle requires first a laser induced heat pump process. Heat is withdrawn from a gas isothermally by laser power. Next, at a later time or at a different location, the sum of the heat withdrawn and the laser supplied energy is released isothermally as heat at a relatively high temperature. This heat is then converted into mechanical energy in a thermal engine process, with a certain amount of heat to be rejected, ideally, at Carnot efficiency. The study shows that there exists an operating point at which this rejected heat is just equal to the heat initially withdrawn. Thus the net effect of the coupled heat pump - thermal engine operation is the conversion of one form of entropy-free energy into another, a concept that had already been proposed before,[3,4] although not with details of embodiment. Even if allowance is made for the inevitable losses, viz., those that detract from the ideal Carnot efficiency of conventional engines, such quasi-isentropic engines may be of interest in the future in remote operation because of their efficiency. However, an important requirement is the existence of the postulated heat pump processes.

Suitable heat pump processes have to fulfill the following three conditions: (1) They have to extract a substantial fraction of heat content from the working gas; (2) The process must be applicable to relatively large amounts of gas; and (3) The various energy transfer

processes involved must have durations (relaxation times) suitable for the desired heat transfer operation. Such cooling mechanisms - isothermal as well as adiabatic - have been proposed in the preceding study[2] with a more detailed theory of rotational cooling in diatomic gases, which fulfills the three conditions mentioned. However, since none of these particularly suitable heat pump schemes had been discussed previously in the literature, let alone demonstrated, the next step was the experimental verification of the proposed heat pump processes. This is the subject of the present contract.

It will be seen from the results that the basic predictions for the proposed laser induced cooling have been verified. For the first time, it is shown that P-line excitation produces cooling, R-line excitation generates heating in pure gases. The addition of nitrogen to carbon monoxide leads to the expected large factor by which heat pump action is increased over that demonstrated in pure CO. The directly measured peaks of heat extraction approach up to 61% of the theoretically predicted values. By comparison with exothermic R-line effects, it is found that secondary effects obscure the initially produced heat changes during the instrument signal response time. Evaluation of these secondary effects then show that the theoretically predicted 11.7% of radiation power is converted into heat extracted, and that in the axis of the irradiated volume temperatures are reduced by up to 44 K. Considerably larger values for heat extraction and temperature reduction can be expected for operation with pulses of longer duration and larger energy.

The results corroborate the assumption that the remote operation of a quasi-isentropic laser engine is in principle possible. Perhaps of more current practical interest is the possibility of a remotely operated heat pump in its own right. A radiation resonance process which can either maintain an isolated remote sample isothermally at a low temperature or substantially cool a gas adiabatically within microseconds may have current or future applications.

2. ROTATIONAL COOLING

A discussion of the expected heat pump effects is now appropriate since these predictions underly the choice of experimental design and procedure.

2.1 Structure and Exchange of Molecular Energies

The mechanism of a laser induced molecular heat pump operating by rotational cooling is based on energy exchange processes that can be understood with the aid of Figure 1. Here quantized energy levels are shown for two selected gases, viz. CO and N_2. In each case, the levels indicated represent the sum of vibrational and rotational energy. The rotational energies form a series of relatively closed spaced levels indicated by the rotational quantum number J (J=0 for zero rotational energy). Similarly the vibrational energies form a series of relatively widely spaced levels with vibrational quantum numbers v (v=0 for the vibrational ground state). Because of their wide spacing, only the first two vibrational levels are shown in Figure 1 for the two gases. For each gas, the difference between the purely vibrational levels can be recognized as the distance between the respective levels at J=0. The additional molecular energies then form the rotational manifold over the J=0 state. The purely rotational energy of a level with quantum number J is given[5] by Eq. 1:

$$E_R = J(J+1)B_v \qquad (1)$$

where B_v is the rotational constant at the vibrational level v (however, the difference between B_o and B_1 is relatively small).

The rotational energies E_R overlap in their range the molecular translational energies $mv^2/2$ in the temperature regions of interest (typically 40 K to 400 K), i.e., they are of the order kT (k the Boltzmann

Curve 745463-A

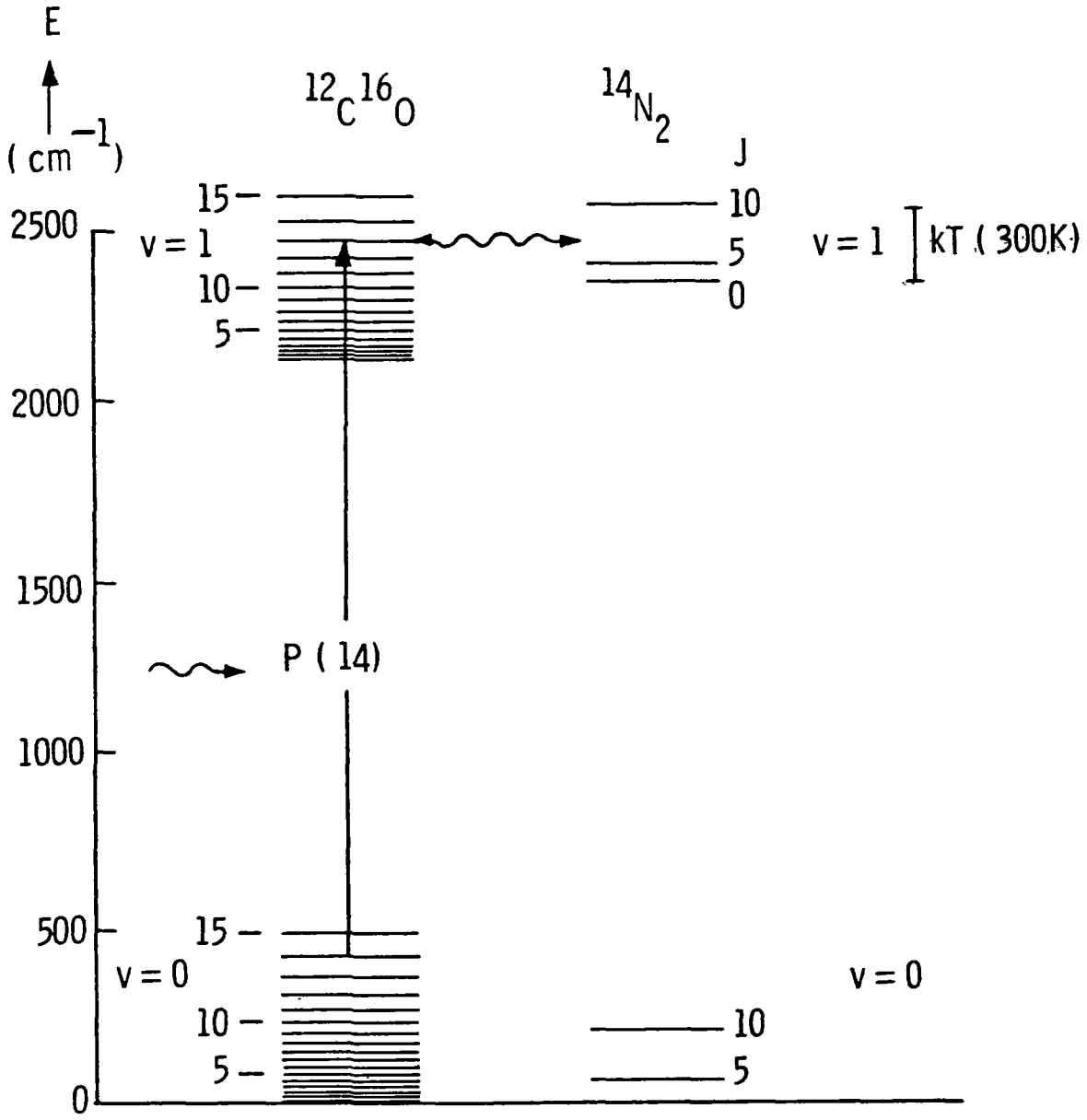

Figure 1. Vibrational-rotational energy levels in CO and N_2.

constant). For this reason, the exchange of rotational and translational energy is very fast and, in fact, occurs at every collision between molecules, whether between CO and N_2, or between molecules at v=0 and v=1 (if populated). Thus there establishes itself very rapidly a thermal equilibrium between rotational and translational energy levels, e.g., within 10^{-10} sec at atmospheric pressures and within 10^{-8} sec at 10 Torr. Thus we speak of a translational-rotational reservoir or heat content. In the language of statistical mechanics, the translational-rotational reservoir represents an ergodic system of molecules.

In contrast, the vibrational energies E_V are large compared to kT (excepting high temperatures, $T > 10^3$ K), at least for the majority of diatomic molecules such as CO and N_2. Normally, then, the vibrational levels above v=0 are not thermally excited and remain (virtually) empty. If, however, resonant radiation or high-energy collisions excite such molecules from v=0 to v=1, they form a population that has a high stability against the strongly exothermic process in which their vibrational energy is converted into translational or rotational energy (VRT). In particular, vibrationally excited CO and N_2 molecules require 10^{10} collisions before that excitation is converted into heat by the VRT process. The vibrational relaxation rate to the R-T reservoir is, therefore 10^{10} times slower than that for the rotational excitation.

This disparity between relaxation times makes it possible for vibrational excitations and rotational-translational energies to coexist, even in the same molecule, for relatively long times. If, in addition, no nonthermal processes shorten the vibrational lifetime (as for instance it is possible in N_2), this coexistence of the two energy populations as quasi-nonergodic systems, lasts $\approx$1 second at atmospheric pressures and about a hundred seconds at 10 Torr. These considerations are important for the cooling processes in question.

2.2 Rotational Heat Pump Processes

Rotational cooling can be effected[2] in single gases and more effectively, in gas mixtures.

We consider first the process in single gases (and first ignore the N_2 term scheme in Figure 1). Absorption of radiation in diatomic molecules by transitions from the vibrational ground state to the level at v=1 is limited to two branches (P and R) of vibrational-rotational lines, arising from the selection rule $\Delta J = \pm 1$. In the P-branch transitions, the rotational energy of a molecule changes from $E_R(J)$ at v=0 to $E_R(J-1)$ at v=1 [cf. Figure 1, where the P(14) transition is shown for the CO energy term scheme]. The rotational energy of the molecule, therefore, suffers a net loss which follows from Eq. (1) as

$$\Delta E_R = -(B_o+B_1)J - (B_o-B_1)J^2; \quad J = 1,2.....[\text{P-Lines}] \qquad (2)$$

where B_o is the rotational constant of CO for v=0 and B_1 that for v=1 and are known to be[5], in spectroscopic units,*

$$B_o = 1.9225 \text{ cm}^{-1} \quad \text{and} \quad B_1 = 1.9050 \text{ cm}^{-1}. \qquad (3)$$

Introduction of these values into Eq. (2) then yields for the rotational loss per molecule by absorption of the P(14) line (i.e., J=14):

$$\Delta E_R = -57.00 \text{ cm}^{-1} = -113.19\ 10^{-16} \text{ erg} \quad [\text{P(14) line}] \qquad (4)$$

with conversion* from cm^{-1} to erg.

In diatomic gases at temperatures in the range of interest, the mean of the thermal energy or heat content per molecule (which includes a rotational and a translational part) amounts to (5/2)kT. At T=300 K, this amounts to $1035 \cdot 10^{-16}$erg. A comparison with Eq. (4) shows then that a CO molecule undergoing a P(14) transition by absorption loses 10.9% of the thermal energy that it has in the average under the equipartition law. If a gas column of CO absorbs N photons of radiation at resonance with the P(14) transition at (2,086.323 cm^{-1}) an amount of heat equal to $N \cdot \Delta E_R$ will be withdrawn from the column within 10^{-8} sec at 10 Torr, while the high vibrational energy remains undisturbed until other processes may release it.

---

*Spectroscopic convention uses the wavenumber $\tilde{\nu}$ in [cm^{-1}], which is the number of wavelengths per cm in vacuo, as a measure of frequency in [Hz], i.e. $\nu = c\ \tilde{\nu}$ ($c=2.9979 \cdot 10^{10}$ cm sec^{-1} speed of light in vacuo). With Planck's relationship of energy, $E=h\nu$(Planck's constant $h=6.6256 \cdot 10^{-27}$ erg·sec), the wavenumber is also a measure of molecular energy, viz., $E=hc\tilde{\nu}$. Thus 1 $\text{cm}^{-1}=1.9863 \cdot 10^{-16}$erg. The molecular structure energies in [cm^{-1}] can be compared with molecular thermal energies in terms of kT with $k = 1.3805 \cdot 10^{-16}$erg deg^{-1}.

In contrast, R-line absorptions produce heating since in the vibrational transition they elevate the rotational quantum number of J to J+1 so that the exciting photon provides an excess of energy which is taken up by the rotational heat content. This excess energy is computed, in analogy to Eq. (2), from Eq. (1) and yields

$$\Delta E_R = 2B_1 + (3B_1 - B_o)J - (B_o - B_1)J^2; \quad J=0,1...[\text{R-Lines}]. \quad (5)$$

P-line cooling and R-line heating, which occur in every such absorption process, had apparently not been considered before it was suggested for isentropic energy conversion cycles.[1,2] However, more recently, use of P-line cooling has been proposed also elsewhere in the literature.[6]

A second method of rotational cooling involves gas mixtures. In single gases, the rotational selection rule, $\Delta J = \pm 1$, limits rotational heat extraction to a relatively small difference in rotational heat content. How much more can be obtained by extracting the full rotational energy, or at least a large fraction of it, from a molecule at level J, can be appreciated by comparing Eqs. (1) and (2). For example at levels v=0, J=14, a CO molecule has according to Eq.(1) the rotational energy $E_R = 403.7\ cm^{-1}$, whereas according to Eq. (4), the differential energy created by the P(14) line is only $\Delta E_R = 57.0\ cm^{-1}$. However, this inhibition by the selection rule can be circumvened by adding to the absorbing gas a comparably much larger amount of a diatomic host gas, provided that the latter has a suitably higher first vibrational level than the absorbing gas. It can be seen from Figure 1, with an especially simple example, how such a combination can enhance the cooling process. If a CO molecule absorbs a photon resonant with the P(10) transition, the resulting heat extraction amounts to $-40.02\ cm^{-1}$ as can be found by using Eqs. (2) and (3). However, in a collision with an N_2 molecule, the excited CO molecule is very likely to transfer its vibrational energy to it, so that CO transits from v=1 to v=0 and N_2 from v=0 to v=1. As shown in Figure 1, the upper level of the CO transition (v=1, J=9) is nearly coincident with the level (v=1, J=0) of N_2. In this particular example, the energy net balance is thus the removal of the full rotational energy of CO at the level (v=0, J=10) to form,

with addition of the P(10) photon energy, a vibrationally excited N_2 molecule in the lowest rotational state. Thus heat of approximately $-211.5\ cm^{-1}$ is extracted from the gas mixture [cf. Eq. (1)].

Such resonance energy transfer between molecules of the same or different species, as described, occurs with a high probability, if the exchanging levels differ in energy by kT or less. Quite generally, if resonance energy is transferred from a molecule I in the first vibrational state to a molecule II raising it to v=1, the thermal energy withdrawn is

$$\Delta E = E^{I}(1,0) - E^{II}(1,0) + \Delta E_R^I \quad . \tag{6}$$

Here $E^I(1,0)$ is the purely vibrational energy (i.e., v=1, J=0) of the absorbing molecule, amounting in CO to $2143.27\ cm^{-1}$; $E^{II}(1,0)$ is the corresponding energy in the second gas, amounting in N_2 to $2330.72\ cm^{-1}$; and ΔE_R^I represents the change in rotational energy in the absorption transition of the first gas, as given for P-lines by Eq. (2) and for R-lines by Eq. (5). The energy ΔE in Eq. (6) is in the general case less than the full rotational energy E_R^I. For example, P(14) excitation of CO with subsequent transfer to N_2 withdraws heat in the amount of $244.45\ cm^{-1}$, as can be found with Eq. (6). This amount is only 61% of the CO rotational energy in the (v=0,J=14) state, although it is still by a factor of 4.2, larger than the heat extraction effect obtainable from the P(14) transition in the single gas. Since the frequency of the P(14) line is $2086.32\ cm^{-1}$, 11.7% of the pump power is converted into heat extracted.

2.3 Secondary Effects in Molecular Heat Pump Operation

The primary cooling process by which a (rotational-translational) thermal equilibrium establishes itself within the volume traversed by the pump beam occurs in the molecular collision time, i.e., within one nanosecond at 100 Torr, in a single gas. The thermalization time of a gas mixture, however, is longer. In CO/N_2 mixtures at 100 Torr, that time may be as long as 22 μsec, although resonance energy transfer times are expected to be much shorter. Subsequent to the initial cooling, certain secondary processes have to be expected as follows:

(1) Spontaneous Emission. The absorbing molecules may reemit their vibrational energy as fluorescence. This occurs with a characteristic radiative lifetime which for CO is 30 msec. The process is important for removal of the vibrational energy without gas heating by (VRT) collisions. N_2 neither absorbs nor emits infrared radiation since it lacks an (ionic) dipole moment. However, in mixtures with CO, it prolongs the reradiation process since it acts as storage medium of the vibrational energy.

(2) V^*V^* Energy Transfer. Vibrationally excited CO molecules (CO*) may exchange energy in collisions so that, for example, two molecules at v=1, separate with one molecule in the vibrational ground state, v=0, the other excited to v=2. This is an exothermic process which will be in detail described along with the experimental results.

(3) Diffusion. With drift velocities inversely proportional to pressure, molecules diffuse through the gas volume outside the irradiation column to the walls. If the diffusion time to the walls is of the order of the radiative lifetime, or shorter, excited molecules may arrive with their vibrational energy still intact. It is not known, a priori, what fraction of such wall collisions effects the release of the vibrational energy as heat. An answer may be expected from the experiments.

(4) Heat Conduction Through the Gas and to the Walls. Although thermal conductivities are practically independent of gas pressure, the diffusivity effect becomes important for small pressures since the smaller heat capacity results in a smaller thermal time constant.

(5) VRT Collisions. If vibrational energy, by a collision of the molecule, is converted into rotational-translational energies, the heat produced is an order of magnitude larger than the heat extracted in the mixed-gas process. Although an N_2 or CO molecule requires 10^{10} collisions with other CO or N_2 molecules for a VRT process to occur, collisions with polyatomic molecules like CO_2 or H_2O act faster by many orders of magnitudes. Thus gaseous impurities have to be kept below certain pre-

determinable levels in the experiments.

The phenomena and expected effects described here present the basis for the choice of experimental design and measurements.

3. EXPERIMENTAL DESIGN AND PROCEDURES

3.1 Apparatus

The equipment used for the measurements was constructed under Contract NAS 2-10078 with NASA-Ames. The Final Report[7] under that contract describes in detail the considerations which determined the choice of components and design dimensions. Therefore, a brief description of the apparatus will suffice here, emphasizing those features which are important for the interpretation of the measurement results.

The experimental arrangement is shown in Figure 2. A Lumonix CO_2 Laser Model 203 (not shown) produces a beam with a Gaussian distribution of the radial intensity profile (TEM_{oo} mode). The laser emission is pulsed at the rate of 0.5 - 2 Hz, but only single pulses were used. The beam is incident on a crystal of Tl_3AsSe_3 (TAS), a nonlinear material which at the proper phase match angle doubles the frequency of the laser radiation. Millijoules of pulse energy could be obtained in this second harmonic generation (SHG). Further details on this radiation source (a change from original plans) are described in Section 3.3.

For most measurements the laser was tuned to the P(24) line of the CO_2 (00°1)-(02°0) band, generating, as indicated in Figure 2, a wavelength of 9.6 μm which is converted to 4.8 μm by the SHG crystal. The exact second harmonic frequency of the P(24) line is 2086.326 cm^{-1} and, therefore, in excellent fortuitous coincidence, well within the Doppler line width, with the P(14) line at 2086.323 cm^{-1} of the CO fundamental absorption band. According to Section 2.2, P-line absorption is expected to produce cooling, and the P(14) frequency-line is the only one with which the frequencies of any other CO_2 line can be brought into coincidence after doubling. There exist, however, two coincidences for R-lines. The frequency doubled CO_2 R(18) line of the (00°1) - (02°0)

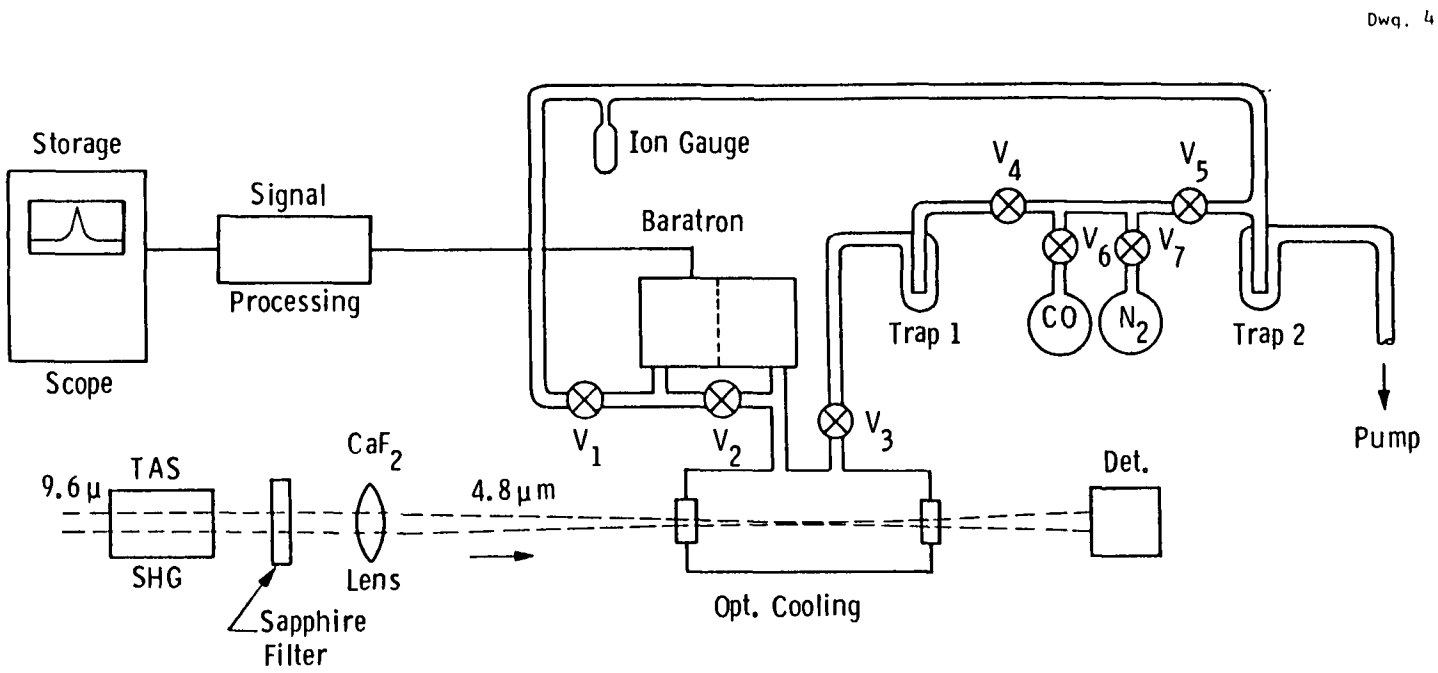

Figure 2. Schematic of the experimental arrangement.

band at 2154.605 cm^{-1} coincides well with the fundamental R(2) line of CO at 2154.598 cm^{-1}, and the frequency doubled CO_2 line R(30) of the (00°1) - (02°0) band at 2169.270 cm^{-1} has a still useful, although marginal, overlap with the fundamental R(6) line of CO at 2169.200 cm^{-1}. Since the R-lines are exothermic, they are important for comparison with the endothermic P-line.

After adjusting the crystal to the phase match angle, while simultaneous aligning the SHG beam with the fixed axis of the optical gas cell, any of the three P-or R-lines could be applied without further realignment except for the tuning of the laser grating. The fundamental pump beam component (near 9.6 μm) exiting from the TAS crystal is blocked by a sapphire filter, while the harmonic component (near 4.8 μm) proceeds to a CaF_2 lens. The beam spot size as a function of distance from the lens was determined by measuring the pulse energy through small apertures of various diameters. It was thus found that the beam waist in the center of the optical gas cell was 1.0 mm in diameter.

The optical gas cell, in which the laser beam produces the thermal effects to be studied, is a copper cylinder of 11.5 cm length and 2.22 cm inner diameter sealed at its two ends by Ceramasil sapphire windows. The choice of the diameter represents a compromise between the need for a small volume to obtain a good pressure response and the requirement of extending the diffusion times to the walls at the pressures of interest. The inner walls of the cell were mechanically roughened and painted with Aquadag (Acheson Colloids Co.), a graphite suspension which, after baking, effectively absorbs radiation in the 4-5 μm range. Smooth, specularly reflecting copper walls would imprison the spontaneous emission of the excited CO molecules. Although the average effect of the randomized P - and R-branch emissions on temperature could be ignored, the prolonged presence of photons of the fundamental CO band would complicate the interpretation of the observed time-variant phenomena. Furthermore, since the heat capacity of the copper cell is about 10^6 times larger than that of the enclosed gas, radiation absorption at the walls has no more effect on the adiabatically conducted measurements than radiation incidence on walls which are completely transparent.

The gas handling system, shown in Figure 2, is first baked at 200-250°C, evacuated to 10^{-8} Torr and, after gases have been admitted to the volume between Nupro Valves V_1 and V_5, held outside these valves to 10^{-7} Torr during a normal course of the measurements. The gas supply in Matheson Research Grade Flasks consists of 99.99% pure CO and 99.998% pure N_2. These measures are taken to ensure that the VRT rate contributed by gaseous impurities, is still smaller than that of CO and N_2. The valve system shown in Fig. 2 proved to be adequate for filling the optical cell with any desired combination of partial CO and N_2, while keeping the need for the removal of excess gas by evacuation to a minimum.

3.2 Measurement Procedures

The thermal effects in the gas cell are measured by the pressure changes produced in the closed volume between Valves V_2 and V_3 and registered by the baratron. The latter (MKS Model 315) determines the pressure differential between two chambers of small volume (2 cc) separated by a tautly stretched diaphragm. The signal is taken capacitively from the displacement of the diaphragm caused by the pressure difference and, after processing, displayed on a storage scope (Tektronix Model 7633 Oscilloscope). The baratron system used also includes a digital readout unit with which pressure differences can be measured that are static or vary slowly (1/2 sec or more). As a compromise between accuracy and convenience, the differential pressure range was chosen as 0-10 Torr. This permits the measurement of the static cell pressure up to 10 Torr relative to vacuum (by opening Valve V_1). The higher cell pressures are measured by filling the cell in steps of 10 Torr, or less, and alternatively opening and closing Valve V_2 (V_1 closed), keeping count of the cumulative pressure buildup with corrections for the small volume increase after opening V_2. For maximum accuracy, dynamic pressures are always measured with zero differential of the static pressures.

The dynamic pressure differential ΔP is directly a measure of the net amount of heat extracted from, or contributed to, the gas in the

cell volume V at any one time, independent of the static temperature T, the static pressure P, and the diameter of the pump beam. This follows from the basic (ideal) gas laws.

If a negative or positive amount ΔQ of heat is added to the gas (specifically to its rotational-translational molecular energies) in some arbitrary distribution, there will result a mean change $\overline{\Delta T}$ of the gas temperature. This in turn produces a pressure change ΔP:

$$\Delta P = \frac{P}{T} \overline{\Delta T} = \frac{P}{T} \frac{\Delta Q}{C_V} \tag{7}$$

Here C_V is the heat capacity of the gas at constant volume V. C_V is calculated from gas statistical data, viz. the specific heat of a diatomic molecule equals (5/2)k, and there are, per unit volume, Loschmidt's number $n_o = 2.687.10^{19}$ cm^{-3} of molecules at N.T.P.*, so that at the temperature T[K] and the pressure P[Torr]

$$C_V = \frac{5}{2} n_o k \frac{273.2}{760} \frac{P}{T} V = 3.333\ 10^{-4} \frac{PV}{T} \ [J\ deg^{-1}] \ . \tag{8}$$

Introduced into Eq. (7), this yields

$$\Delta P = 3.00 \cdot 10^3 \frac{\Delta Q}{V} \ [Torr\ cm^3 J^{-1}] \tag{9}$$

where ΔQ (in Joules) is the fraction of absorbed radiation energy converted into heat. Thus the pressure change is a direct measure of the heat extracted or added, with the gas volume V as the only parameter. These relationships remain valid for any $\overline{\Delta T}$ and ΔP that do not produce a gas condition exceeding the limits of the ideal gas laws.

The response of the baratron to a dynamic pressure change is a voltage signal which is delayed in time by the electromechanical pick-up process. It will be seen in Section 4 that all predicted energy transfer processes with their resulting heat contributions do indeed occur. Although these processes have distinct relaxation times, they partially overlap. Where exact quantitative accounting is necessary, the analytical process of unfolding or separation by other means has to be carried through.

*i.e., T = 273.2 K; P = 1 atm.

3.3 Changes in Ancillary Equipment

It appears appropriate to conclude the section on the experimental arrangement with an account of changes that had to be made in the radiation source accessories since these changes necessitated a considerable extension of contract time, although not of cost.

It had originally been planned[7] to use, as frequency doubler, a small $CdGeAs_3$ crystal obtained by courtesy of A. Mooradian's group at the MIT-Lincoln Laboratories. The very high demonstrated efficiency of this material[8] would have made it possible to use this material in combination with a 200 Watt cw CO_2 laser. Such an operation is expected to be particularly suitable for the mixed gas cooling process (see Section 2.2) since it would provide adequate time for the transfer of vibrational energy from CO to a large fraction of N_2 molecules (see Section 2.3). However, repeated microscopic inspection revealed that the $CdGeAs_3$ crystal had developed fine cracks that appeared to grow spontaneously with time. It seemed inadvisable to expose the crystal to the risk of further cracking by high power irradiation. Other crystals of $CdGeAs_3$ were not available because of their exceedingly difficult growth conditions even in small sizes.

Therefore, as a fall-back alternative Tl_3AsSe_3 (TAS) had to be used. To achieve the necessary conversion efficiency, large fundamental peak powers were needed, and the apparatus shown in Figure 2 was transferred to a location where a Lumonix CO_2 laser was available. About a decade before, TAS had been developed at Westinghouse and its nonlinear capabilities, especially with respect to SHG, demonstrated.[9] Since that time, TAS crystals have been under steady development for use as acousto-optical tunable filters(AOTF) and, more recently, also for second harmonic generation. However, it was not until the middle of 1983 that a crystal was made available with a harmonic power output sufficient to carry out the measurements reported here.

4. EXPERIMENTAL RESULTS

This section describes the phenomena observed under various experimental conditions. The description is, at first, qualitative. A quantitative evaluation of any single observation is not possible until all other effects have been explained which may contribute to the signal to the extent of their relaxation times. The quantitative evaluation of the measurements presented in this section is contained, to the extent possible, in Section 5.

4.1 Thermal Effects Induced in Pure CO

The experiments are reported more or less in their chronological order. The interactions in pure CO were dealt with first since they were expected to present a simpler situation than the case of CO/N_2.

4.1.1 P-Line Cooling and R-Line Heating

Figure 3 shows (a) the endothermic effect of P-line absorption and (b) the exothermic effect of R-line absorption at about 9 Torr. It was convenient to generate a positive signal for pressure reduction, i.e., for cooling, in the optical gas cell. As described in Section 3.1, P(14) is the only P-transition that can be brought into resonance with the second harmonic of a CO_2 line. Among the R-lines, R(6) generates a trace similar to that of the R(2) line used for Figure 3 (b).

The existence of these thermal effects in P- and R-transitions has been little noticed before and, to our knowledge, has not been demonstrated before.

The decay of the thermal pulses had been expected as the result of conduction to the walls. On the other hand, the slope in the rise of the pulses may be interpreted, at this stage, either as caused by the

HEATING → COOLING

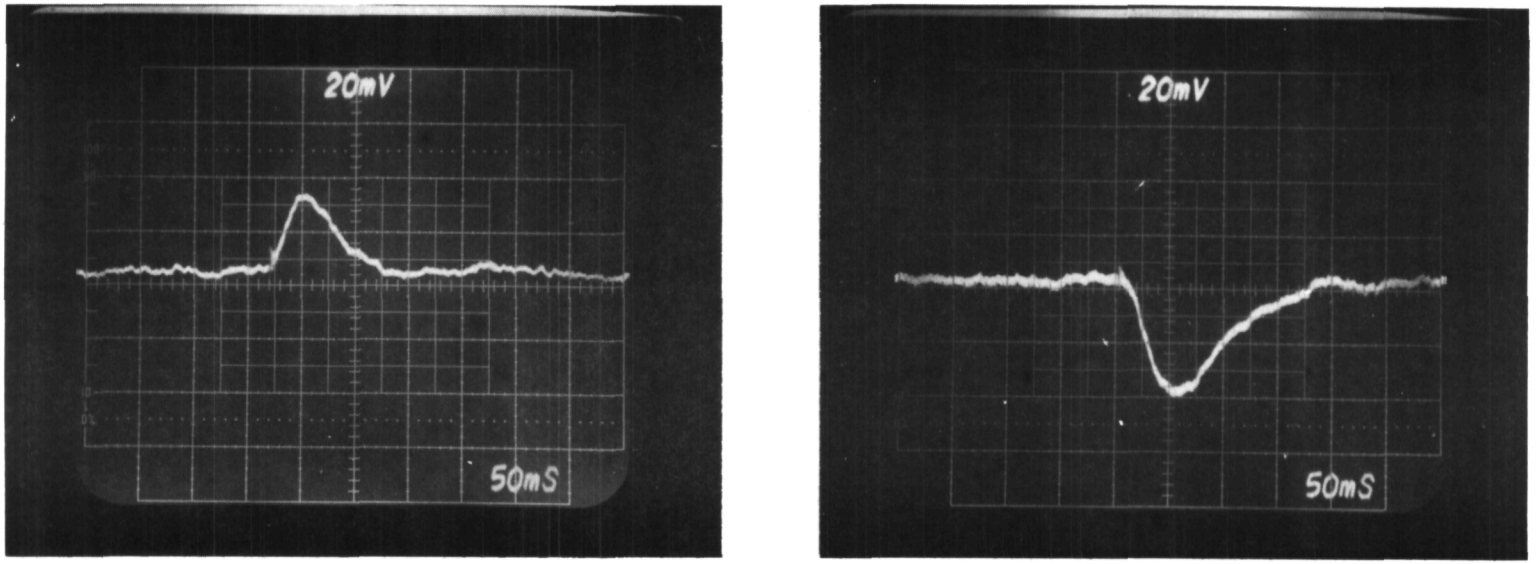

a b

Figure 3. Thermal effects due to P-line and R-line absorption in pure $^{12}C^{16}O$ at 9.2 Torr:
(a) P(14), v = 0 → v = 1 at 2086.323 cm^{-1} produces cooling.
(b) R(2), v = 0 → v = 1 at 2154.598 cm^{-1} produces heating.

response time of the baratron or by the interaction of excited CO molecules, or both.

4.1.2 P(14) Effects on CO at Higher Pressures

When at nearly constant radiation pulse energy, at resonance with P(14), the CO pressure is raised above about 12 Torr, the cooling peak is followed by a heating cycle with a peak that indicates a larger amount of heat generated than was before withdrawn. This behavior was followed up by increasing the CO pressure in steps to about 130 Torr. Two of these measurements are shown in Figure 4, viz., (a) at about 18 Torr and (b) at about 55 Torr (note the different scales per large division for voltage as well as time and note also that the occasional small vertical noise spikes are caused by the spark gap of the Lumonix laser). It is found that, while the initial cooling peak persists, subsequent heating increases with pressure up to about a signal of 1.5 V at 100 Torr, but from thereon decreases somewhat. The heat signal at 1.5V is 75-50 times larger than the heat extraction signal at 20-30 mV found for the lower pressures. The heat extracted by the P(14) transition is $-57.00\ cm^{-1}$ according to Eq. (4) and therefore represents a 2.73% of the P(14) photon energy of $2086.3\ cm^{-1}$. The signal peak reached in cooling is, of course depressed by secondary effects (as is to a lesser extent that of heating) so that the peak ratio will be less than 50. Nevertheless, it appears that the heat peak indicates a large percentage, or even a complete, conversion of the photon energy into heat.

Such a conversion is possible only by one of two qualifying processes. The first is VRT transfer by molecular collisions, which increase in their rate linearly with pressure so that this rate can compete successfully with those of spontaneous emission and diffusion This interpretation is, however, at once contradicted by the experiment: as seen in Figure 4, a pressure increase by a factor 3 produces a heat peak increase by a factor 10. Aside from that, the (VRT) relaxation time in 55 Torr CO is expected to be about 10 sec , rather than the 50 msec observed. The second possible process is (VV) energy exchange between

a

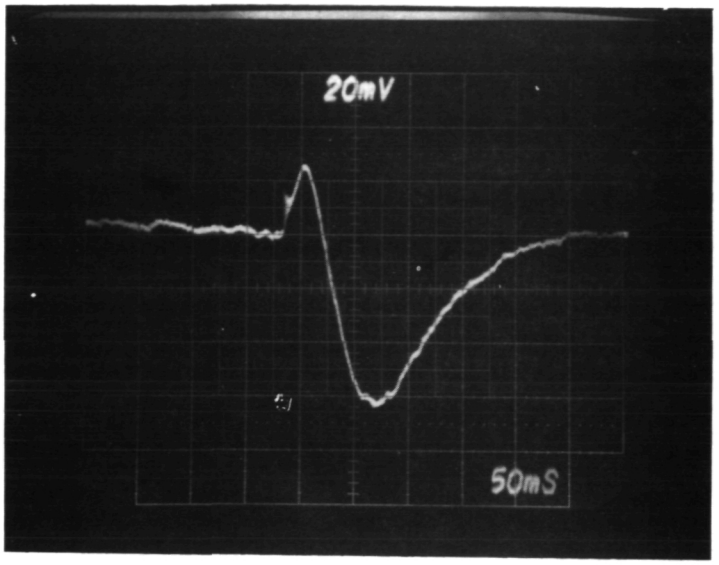

b

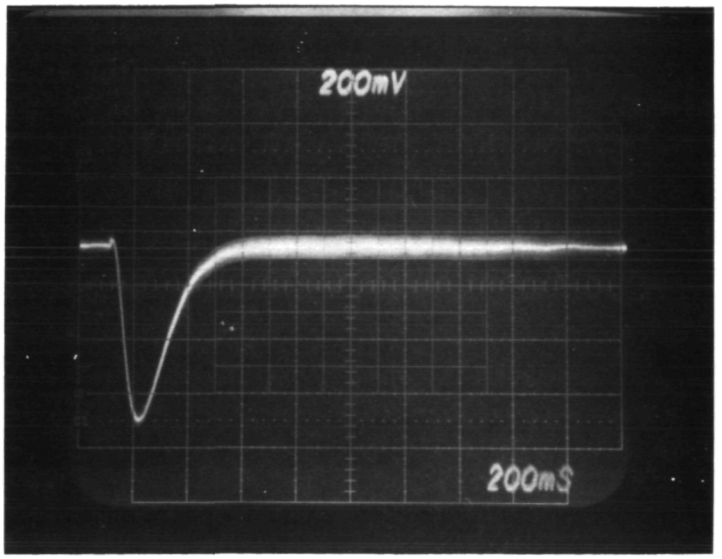

Figure 4. Thermal effects of P(14) irradiation on CO at higher pressures: (a) 18.3 Torr. (b) 54.9 Torr. Cooling (above base line) is followed by heating (below base line).

vibrationally excited molecules [see Section 2.3 (2)]. This is an exothermic binary process with a rate which should increase with the square of the number density of the vibrationally excited molecules. On first sight, this second interpretation seems to fail too, since the total number of molecules excited to v=1 is equal to the number of absorbed photons, and this number increases only slowly with gas pressure because more photons are absorbed in the cell volume. However, this idea has only to be carried further. The length over which a certain fraction of incident radiation is absorbed is inversely proportional to the gas density. Therefore, not only has the number of photons absorbed somewhat increased, but the number density of the vibrationally excited molecules has increased proprotionally to the pressure. Thus the interpretation of the steep increase of generated heat as due to (VV) transfer between excited CO molecules agrees well with the observation that a factor 3 in gas pressure produces a 10-fold increase of the heat peak.

This conclusion was submitted to an experimental test by repeating the experiments just described with an unfocused pump beam at the same pressures. The vibrationally excited molecules initially created in the 1 mm diameter column of the focused beam in the cell center diffuse to a diameter of 3 mm at 100 Torr, and more at lower pressures, after 40 msec. Nevertheless, if by removal or displacement of the CaF_2 lens (see Figure 2) the beam becomes unfocused, it will propagate through the cell with a larger cross sectional area and generate excited CO molecules with lower density. Hence one should expect lower heat production. The result of this experiment is shown by two examples in Figure 5 for which the conditions, except for focusing, have been preserved as in Figure 4. Figure 5a, for which the lens had been moved directly in front of the cell entrance window, shows a heat excursion which is numerically almost equal to that of cooling. In contrast, the corresponding trace for the focused beam [Figure 4 (a)] shows a heating pulse 2.4 times larger than the cooling peak. The CaF_2 lens had been removed for the case of Figure 5 (b) which shows for 55 Torr a heat signal peak* of 100 mV and a cooling peak of about 20 mV for a ratio of 5:1, whereas the

*Note in proof: Vertical scales(mV/div) Fig.5b-50; Fig. 6a-20; Fig. 6b-100.

a

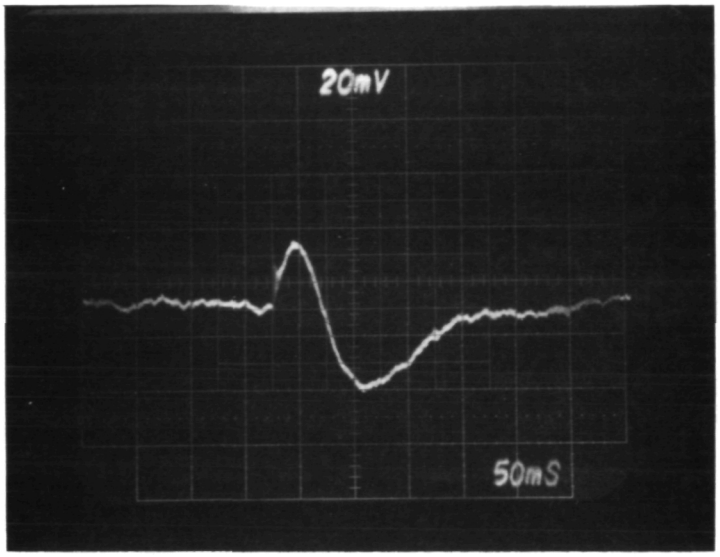

b

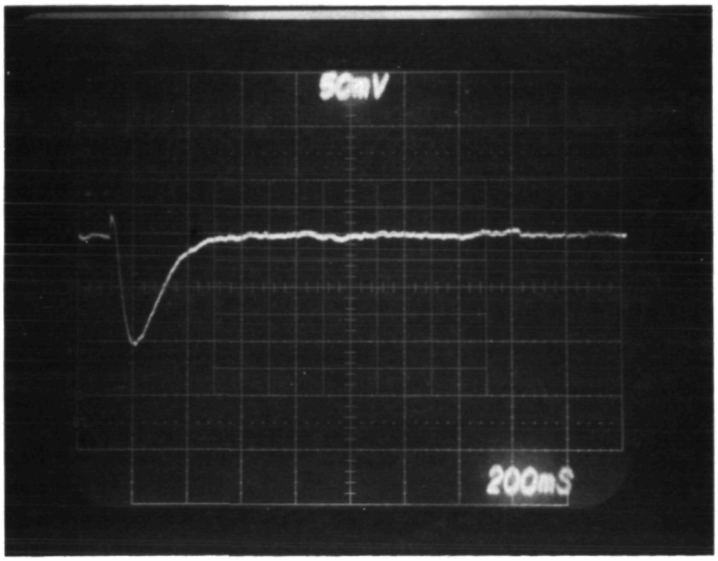

Figure 5. Thermal effects of P(14) irradiation with unfocused beam: (a) 18.3 Torr. (b) 54.9 Torr. Compared with Figure 4, the ratio of heating to cooling is reduced, indicating a CO*/CO* vibrational exchange.

corresponding ratio in Figure 4 is in the order of 30:1. Thus the decrease of the heat cycle peaks in their absolute values, as well as in their ratios to the cooling cycle peaks, observed with unfocused irradiation is further confirmation of the assumed (VV) exchange process in CO.

4.2 Cooling Effects in CO/N_2 Mixtures

As discussed in Section 2.2, the mixed gas cooling process has been proposed as a method of extracting a much larger fraction of rotational heat than is possible with P-line cooling. In the case of CO/N_2 mixtures, an additional advantage is important. The experiments described in Section 4.1.2 have revealed the surprisingly strong effect of the exothermic (VV) process in CO on the degradation of P-line cooling. The additional advantage of N_2 mixed with CO is that a CO molecule can transfer its vibrational energy to N_2 before it has an exothermic collision with another excited CO molecule.

These expectations are borne out by the traces shown in Figure 6, initiated with P(14) resonance radiation. For a partial pressure of 9.7 Torr CO and of 8.9 Torr N_2, Figure 6(a) shows a cooling peak of 120 mV. This should be compared with the results obtained with about the same pump energy for pure CO. Figure 3 (a) yields for 9.2 Torr CO a cooling peak of about 28 mV so that the addition of approximately the same partial pressure of N_2 yields a signal increase by a factor of 4.3. The total pressure in the conditions presented in Figure 6 (a) is nearly the same as for pure CO in Figure 4 (a), but in contrast to the latter, the heat peak is entirely absent.

As seen in Figure 6 (b), increase of the N_2 pressure to 92.5 Torr at 8.4 Torr CO yields a cooling peak of 600 mV. This is more than 21 times larger than in the pure CO case depicted in Figure 3 (a). Since, according to Section 2.2, the quantum efficiency for cooling in the mixed gas is 4.29 times larger than in pure CO, an additional factor of 5.0 must be attributed to the elimination of the CO^*/CO^* processes as well as to an increase of the conduction time to the walls at the total pressure of 100 Torr. The effect of the smaller conduction rate is also dis-

a

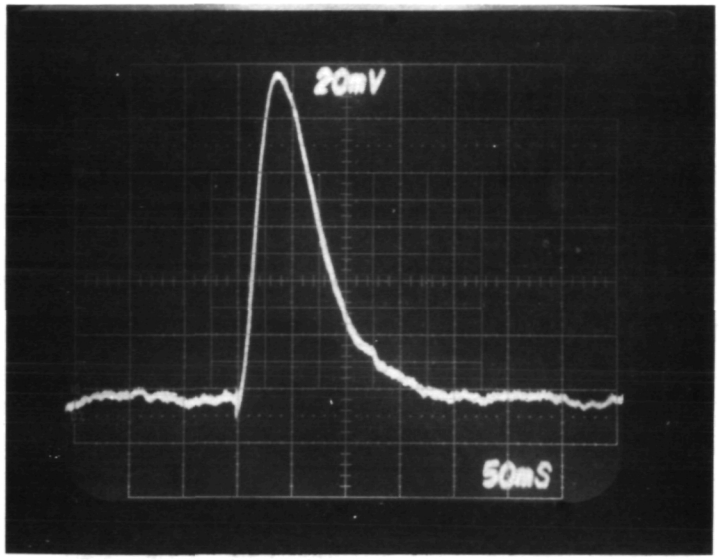

b

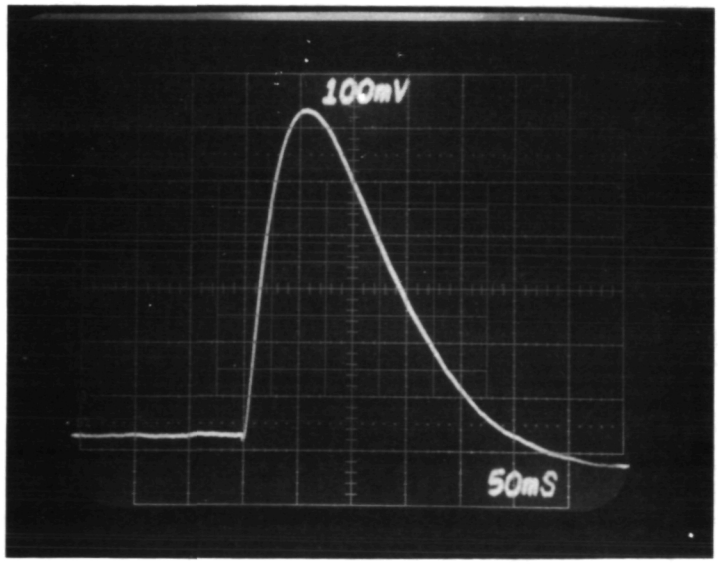

Figure 6. Cooling effect in CO/N_2 mixtures: (a) 9.7 Torr CO; 8.9 Torr N_2. (b) 8.4 Torr CO, 92.5 Torr N_2. Cooling follows absorption of P(14) line by CO.

played by the slower return of the trace to the base line compared to that shown in Figure 6 (a).

Further inspection of Figure 6 (b) shows that net heat is developed 250 msec after the start of the cooling pulse. Traces taken of the pulse with expanded time scale (not shown in this report) reveal that a heat maximum of 40 mV occurs 360 msec after the start of the cooling trace. Interpretation of this feature is presented in Section 5. The trace returns to the base line 400 msec after the heat maximum.

When the nitrogen pressure is further increased, the amount of heat extracted for a given number of photons absorbed reaches saturation. This limit represents the condition that essentially all the vibrational energy of CO, serving as "doping" gas, has been transferred to N_2, i.e., the host gas. An example is shown in Figure 7 (a) for 7.7 Torr CO mixed with 202.7 Torr N_2. Here the cooling pulse signal reaches a peak of 614 mV (the small relative increase is not a fluctuation since it is reproducible as the average of all measurements). The cooling cycle is followed by net heat development with a peak signal of 417 mV about 450 msec after the start of the cooling cycle. The heat signal relaxes to the base line after 1.4 sec (from exposures at longer time scales not shown here).

The experiment just described was repeated with radiation resonant at the R(6) line. The upper level of this transition at v=1, J=7 of CO lies below the v=1, J=0 level of N_2 (see Figure 1).

The result of pumping the same gas mixture used for Figure 7 (a) with an R-line is shown in Figure 7 (b). Here a cooling peak of 115 mV is followed by a heating cycle with a maximum at 330 mV, 350 msec after the start of the cooling cycle. The fact that a still substantial cooling effect is produced at all represents the most direct proof of vibrational energy transfer from CO to N_2. No conceivable alternative interpretation could otherwise explain why the exothermic R(6) line can extract heat. The cooling peak is, nevertheless, considerably smaller than the case represented in Figure 7 (a), and this for two reasons. First, the change from the endothermic P(14) transition to the exothermic R(6) transition

a

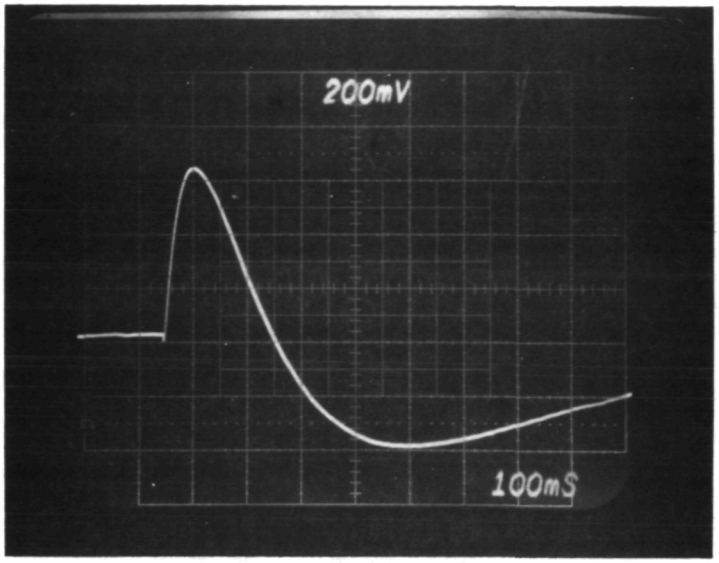

b

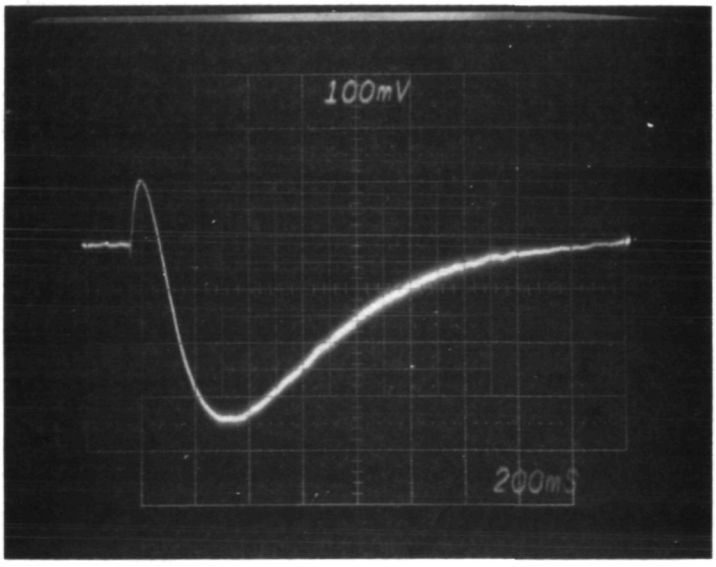

Figure 7. Thermal effects in 7.7 Torr CO mixed with 202.7 Torr N_2 following absorption: (a) by the CO P(14) line; (b) by the CO R(6) line.

reduces the heat amount withdrawn to 66% of the former, as can be verified with Eqs. (3), (4), and (6). Second, less energy was absorbed by the R(6) line from the pump beam since resonance coincidence is marginal as mentioned in Section 3.1. For the same reason the heat peak is lower. Questions of the behavior with time are a subject taken up in the next section.

5. QUANTITATIVE EVALUATIONS

Section 4 has described the experimental results qualitatively, comparing the observed features as to relative orders of magnitude. In this section, it will be attempted to present the absolute magnitude of the thermal effects and of the other observed secondary effects.

Inspection of the traces in Figures 3-7 shows them to consist of two or, at the higher pressures, of three branches. The first branch proceeds to a maximum of cooling or heating. The maximum signal displayed is not the "true" value of heat change achieved in a time considerably less than a millisecond. During the response time of the measurement, detracting effects, notably heat conduction to the walls, reduce the signal before its maximum is reached. Nevertheless, in the evaluation process we begin with the displayed maximum and correct later for the deficit caused by the secondary effects.

The second branch descends from the maximum, signifying a process by which the radiation induced heat change relaxes further. At low pressures, the gas temperature returns directly to the base line, i.e., the static pressure and temperature. This process is caused by heat conduction, but is usually aided by other secondary effects. At higher pressures, these secondary effects become dominant so that, in particular, after an original net cooling, a second maximum of net heating results.

The third branch is the return from the second maximum, (always of heating) to the baseline. This cycle is dominated by heat conduction, although it may be modified by yet other secondary processes.

Obviously it is not possible to quantify any of the thermal effects without taking account of all other competing phenomena which overlap them in time. Only if the whole picture is understood, is it

possible to predict which conditions will allow an upward scaling of the molecular heat pump performance.

5.1 Heat Pump Efficiencies and Temperatures

The purpose of measuring heat extraction and temperatures is not primarily to verify that the predicted cooling occurs in the theoretical amount. It is obvious on the basis of energy conservation, at least in the case of single diatomic gases, that if a transition involves a rotational energy change, cooling or heating must occur, provided that transfer processes between rotation and translation (for all vibrational levels) is fast compared to (VRT) processes. There are, however, the secondary effects, which within certain relaxation times alter the results of these thermal effects, especially in the case of cooling. Therefore, the major purpose of the measurements is to assess the effect of this secondary interference and to determine the means by which such effects can be minimized or, alternatively, utilized.

Comparisons of the experimental results with theory are possible by means of Eq. (9) which yields the pressure change ΔP predicted to result from a heat input (positive or negative) ΔQ. That heat input is the fraction ηE_A of the total energy E_A absorbed by the gas from the pump beam, where the efficiency η equals the quantum efficiency η_q, if secondary effects are absent. Thus with Eq. (9) one obtains

$$\Delta P = 3.00 \times 10^3 \, \eta E_A / V \quad [\text{Torr cm}^3 \, \text{J}^{-1}] \qquad (10)$$

Here the volume equals $V = 54.6$ cm^3, of which approximately 10 cm^3 account for space in the baratron and the tubing to the optical gas cell. E_A, the energy absorbed from the pump pulse by the gas, is determined by measuring the pulse energy in front of, and behind, the cell (with corrections for the effects of reflections from the sapphire windows by comparison with the transmission of the evacuated cell). The pressure change ΔP is obtained from the capacitive signals produced by the baratron such as shown in Figures 3-7 at the scale of 1 mTorr/100 mV. The measurements of E_A and ΔP then yield the efficiency η with Eq. (10).

Table I presents the results derived from these measurements for the gas mixtures listed in Column I. The theoretically predicted ratios of heat extracted to absorbed energy are shown in Column II. For pure CO this ratio is just equal to the P(14) quantum efficiency of cooling, i.e., 2.71%. In the gas mixtures, however, one has to weight the quantum efficiency for cooling of the P(14) absorption and that of N_2 excitation (11.7%) with the concentrations of CO and N_2 in the gas mixture. This is the reason for the efficiency increase with increasing N_2 concentration. Furthermore, a correction is needed for the relaxation of vibrational energy in CO and N_2 by spontaneous emission of CO (N_2 does not radiate in the infrared). Because this particular relaxation process can only use the CO channel, the resulting radiative lifetime τ_R is increased over that of pure CO (30 msec) approximately* to

$$\tau_R = \frac{P_{CO} + P_{N_2}}{P_{CO}} \tau_{CO} \qquad (11)$$

Thus if in the beginning (i.e., at a time after the pulse onset still small compared to τ_R) the total population at v=1 equals N, this number has shrunk to $N \exp(-t/\tau_R)$ after a time t, while $N[1 - \exp(-t/\tau_R)]$ photons of spontaneous CO emission, v=1 →v=0, have left the gas volume. The resulting correction of the heat balance has been applied to Column II for η_{th} at a time t corresponding to the peak of the cooling cycle. The experimental values η_{exp} determined from the peaks of the signal traces with Eq. (10) are shown in Column III. For a comparison between the measured efficiencies, which are reduced from the η_{th} by secondary effects, and the theoretical values, Column IV lists the ratios η_{exp}/η_{th}. The measured efficiencies rise monotonically with increasing N_2/CO pressure ratios up to about 100 Torr N_2, but then level off for reasons explained later.

The comparison between theoretical and experimental values in Table IV shows that whereas the measured efficiencies for pure CO are only 10% of the theoretical values, the addition of an about equal partial pressure of N_2 improves this ratio to 23%. The reason is that such secondary effects as CO^*/CO^* vibrational exchanges and heat flow to the walls are

*Statistical weights of CO and N_2 rotational energies taken to be equal.

TABLE I. Cooling effects produced by a single pulse of about 1.9 mJ absorbed P(14) energy in 1 mm diameter radiation column at various partial pressures of CO and N_2.

I Gas Pressures (Torr)	II $\eta_{th}=\Delta Q/E_{abs}$(theor.)	III $\eta_{exp}=\Delta Q/E_{abs}$(exp)	IV η_{exp}/η_{th}	V $-\Delta T$ (K)	VI $-\Delta T$ (theor. ext.) (K)
9.1 CO	0.0271	0.0027	0.10	1.4*	14
9.7 CO/8.9 N_2	0.0500	0.012	0.23	6*	26
9.4 CO/18.3 N_2	0.0648	0.022	0.34	15	44
9.0 CO/37.0 N_2	0.0814	0.031	0.38	13	34
8.8 CO/54.6 N_2	0.0884	0.041	0.46	12	26
8.4 CO/92.5 N_2	0.0957	0.058	0.61	11	18
8.1 CO/129.2 N_2	0.103	0.055	0.53	7.7	14.5
7.2 CO/202 N_2	0.108	0.057	0.53	5.2	9.8

*corrected for saturation in center of beam.

already much inhibited by N_2 addition. Further increase of the N_2 concentration improves agreement for the same reason until, above about 100 Torr N_2, other secondary effects make their appearance.

Besides the efficiency with which radiation is converted into heat withdrawal, the temperature reduction is of major interest. From Eq. (7) one obtains $\overline{\Delta T}$, the temperature change averaged over the volume V. However, the volume from which the temperature distribution has spread by heat conduction is the gas column of about 1 mm diameter in which about 2 mJ of radiation pulse energy has been absorbed. The significant change in temperature is that which is originally generated in the irradiated space, smaller by a factor of 607 than the volume V. The original temperature change ΔT in the irradiated gas, if restricted to a 1 mm column, is thus

$$\Delta T = 607\ \Delta P\ \frac{T}{P} \qquad (12)$$

where P is the total pressure in the cell. Column V presents values of $-\Delta T$ with values ΔP taken from the peaks of the cooling cycle traces. These measured values, of course, are more or less reduced from the values they had in the beginning, i.e., before the secondary effects reduced them during the response time of the baratron. Correction by theoretical extension of the ΔT values is obtained by dividing the values in Column V by those of Column IV. The resulting temperature changes are listed in Column VI.

The trend of the temperature reductions with increasing N_2 pressure requires several comments. The increasing addition of nitrogen to CO has two opposing effects. First, especially at lower pressures, N_2 increases the cooling efficiency because it inhibits the secondary effects and provides a larger quantum efficiency. On the other hand, increases of N_2 pressure also increase the heat capacity of the gas column and thus decreases the temperature change obtained for the same absorbed radiation energy. This is clearly seen in Column V which shows the measured T values first increasing, then falling.

An important consideration applies to the fact that the measurements presented in Table I were taken with constant absorbed energy of 1.9 mJ. This value is not far from the limit imposed by the pump energy which was available for these measurements. Although 1.9 mJ will saturate pure CO within a beam diameter of 1 mm(0.5 mm spot size), mixtures with relatively high partial pressures of N_2 will be excited to the first vibrational level at a considerably smaller fraction then the limit imposed by saturation. Larger cooling effects than shown in Column VI can be expected at the higher N_2 pressures, if larger pulse energies are applied, necessitating perhaps larger pulse durations.

5.2 Causes of Efficiency Loss

Although Table I shows that the experimentally determined efficiency η_{exp} of heat withdrawal can reach more than 60% of the theoretically expected amount, it is important to examine the causes of the efficiency loss, for several reasons. First, finding the causes may suggest the cure. Second, the information is needed for upward scaling of the desired effects. Third, one can draw conclusions on heat withdrawal, and especially on the temperature, in the irradiation core, in the early part of the cooling cycle which in the experiment is obscured by the delay in signal response of the baratron. In the following, ex-

perimental results are discussed which, although at first sight apparently unrelated to the question, nevertheless go far in answering it.

5.2.1 Heating Effects Induced by R-Line Pumping

If in P-line cooling all secondary effects were absent, the signal would rise, with the delay imposed by the gas-thermometric method, to a constant value (presumably the theoretically expected value). Since it instead passes through a maximum as seen in the traces, we must assume the presence of two secondary detracting effects, viz., heat exchange with the walls and CO^*/CO^* vibrational exchange. Qualitative confirmation of these assumptions is obtained from measurements on R-line heating of pure CO. The significance of this experiment is that the exothermic CO^*/CO^* interactions simulate a higher quantum efficiency of heating by R-line pumping, but a lower quantum efficiency of cooling by P-line pumping. On the other hand, heat exchange with the walls reduces the signal magnitude in either mode of pumping.

The results of the R-line measurements are shown in Table II. There can be no question, because of conservation of energy, that R-line excitation contributes heating in the theoretically expected amount. Nevertheless, inspection of Column V reveals that the efficiencies, measured at the peak of heating fall far short of the theoretically expected values. Thus heat exchange with the walls must play a dominant role in signal reduction. However, in the case of R-line heating, CO^*/CO^* exchange does make a significant contribution in counteracting this effect as seen from a comparison of the results for R(6) and R(2). Since R(2) pumping (because of better frequency coincidence with the CO_2 harmonic) absorbs more than twice the energy of that for R(6), it produces a correspondingly larger concentration of CO^* molecules. The fact that this leads to much better approach of the measured efficiency to the theoretical value than in the case of R(2) signifies that CO^*/CO^* interactions are also important.

One must infer from these results that the efficiency losses for peak cooling of pure CO by P(14) irradiation are indeed caused by

TABLE II. Heating effects produced in 9 Torr pure CO by R-line pumping

I Transition	II Absorbed Energy (mJ)	III η_{th}	IV $\eta_{exp.}$	V η_{exp}/η_{th}
R(6)	0.9	0.012	0.0020	0.17
R(6)	1.0	0.012	0.0021	0.18
R(2)	2.37	0.0052	0.0032	0.61

heat conduction and CO^*/CO^* vibrational transfer. Thus the initial temperature is expected to be close to the theoretically expected value.

5.2.2 Effects of Heat Conduction to the Walls

In the experiment, the cell walls can be considered as a heat reservoir at constant temperature because, compared to the gas they contain, their heat capacity is infinite and their rate of temperature changes virtually zero. The importance of heat conduction to the walls has already been stressed. The time constant τ_H with which heat is exchanged with the walls is the most important feature of this transport process for the observed behavior of signals with time and its interpretation. The time constant is the ratio of the heat content ΔQ of the gas and the rate with which heat is exchanged at the walls. An order of magnitude estimate of τ_H is possible by assuming a radially symmetric temperature distribution and by ignoring the effect of end plates. One thus obtains

$$\tau_H = \frac{C_V \Delta T}{d(\Delta Q)/dt} = \frac{0.5n(5/2k)r^2}{\kappa} \qquad (13)$$

where C_V is the heat capacity of the gas contained in the cylindrical cell, n the number of molecules per cm^3 at the static pressure and temperature, r the radius of the cylinder, and κ the heat conductivity. For T=300 K and r=1 cm, Eq. (13) becomes numerically

$$\tau_H = 5.3 \times 10^{-4} \frac{P}{\kappa} \quad [\text{sec}] \qquad (14)$$

if P is in [Torr] and κ in $[mW \cdot cm^{-1} deg^{-1}]$. At room temperature, $\kappa = 0.25$ for CO and 0.26 for N_2.

From Eq. (14), τ_H = 20 msec for 9.1 Torr of pure CO. If one estimates the system response time at 25 msec, then the signal can follow the initial pressure rise only up to about 29% of its actual value to which the effect of CO^*/CO^* interaction has yet to be added.

For most signal traces the effect of heat conductivity is obscured (folded) by that of other time-variant phenomena. But this complexity

disappears when at high pressures the relaxation to the static pressure is governed only by heat conductivity. An example is shown by Figure 7 (b) for the thermal effect of R(6) absorption in 7.7 Torr CO and 202 Torr N_2. After the initial cooling cycle, three exothermic effects, viz. return of the N_2 energy to CO, (VRT) collisions, and the original R-line penalty, drive the gas to a heating peak, about 350 msec after the start of the pulse. In the latter part of the return trace, the dominant relaxation time should be that of heat conduction. From Eq. (14) one finds τ_H = 428 msec. The slope of the end trace in Figure 7(b), plotted logarithmically, yields τ_H=430 msec. The extent of the agreement with Eq. (14), which is only an estimate, is accidental, but it appears to indicate that after about 800 msec most of the vibrational energy has been given up either as spontaneous emission to the walls or as heat in the (VRT) collisions. Evaluations of the logarithmic slope also shed light on the mechanisms by which the gas relaxes from the point of maximum cooling to the static temperature or to a heat peak. This branch of the trace is of particular interest in the CO/N_2 mixtures because here at least two mechanisms must be active. The first is heat conduction. The second is the refilling of vibrational states in CO after spontaneous emission, whereby the nitrogen v=1 levels return the energy as heat which they had previously withdrawn as enhanced cooling. The time constant resulting from these two effects is calculated by adding the respective decay rates (reciprocals of the time constants) so that

$$\tau^{-1} = \tau_R^{-1} + \tau_H^{-1} \qquad (15)$$

where one obtains τ_R from Eq. (11) and τ_H from Eq. (14). In the case of a 9.7 Torr CO mixture with 8.9 Torr N_2(of Figure 6a), for example, τ_R is 57.5 msec and τ_H is 40 msec with a resulting time constant of 24 msec. Experimentally one finds in this case τ=37 msec from the trace shown in Figure 6 (a). The difference may well be within the error limits or it may be a consequence of the fact that the response time of the calorimetric measurement has been ignored. A deviation in the opposite sense is found in the trace of Figure 6(b) for 8.4 Torr CO and 92.5 Torr N_2. Here τ_R = 360 msec, τ_H = 221 msec for a combined τ =137 msec, whereas the ex-

perimental value turns out to be 81 msec. In the case the instrumental response time can certainly be ignored (and is in the wrong sense), but other effects may add to the heating rate, notably (VRT) exchanges.

5.2.3 Effects of (VRT) Relaxation

The direct conversion of vibrational energy by collisions into heat, i.e., rotational/translational energies (VRT), is a relatively slow process, with a time constant of about 3 sec for N_2 and 1 sec for CO at 760 Torr and proportionally longer at the lower pressures. Nevertheless, if an amount ΔQ has been withdrawn as cooling with a quantum efficiency η, the heat ΔQ_{VRT} returned after a (VRT) process is much larger, viz. $\Delta Q/\eta$. One has thus

$$\frac{\Delta Q_{VRT}}{\Delta Q} = \frac{1}{\eta}\left(1-e^{-\frac{tP}{760\tau_o}}\right) \cong \frac{tP}{760\eta\tau_o} \qquad (16)$$

where τ_o is the (VRT) time constant at 760 Torr, P the pressure in Torr, and the approximation is valid for $tP << 760\tau_o$. Eq. (16) shows that the effect is quite small for the processes occurring at pressures below 100 Torr. However, it explains the heating peaks observed at the higher pressures. For example, in the trace shown in Figure 7 (a), the heating peak equals 31% of the cooling peak, if the latter is extrapolated to the quantum efficiency for which Eq. (16) is valid. On the other hand one expects from (VRT) heating after 400 msec a fraction of 34%. Certain corrections have to be applied to this value, but the end result still agrees with the assumption that the heat peak here is the result of (VRT) collisions. It should also be noted that the relaxation rate from the cooling maximum is significantly increased over that to be expected if radiative relaxation were dominant. The radiative time constant of the CO/N_2 mixture is about 860 msec, but the intervention of the (VRT) process reduces this to the order of 200 msec.

5.2.4 Collisions of Vibrationally Excited Molecules With the Walls

Another potential source of heat generation is the collision of

vibrationally excited molecules with the walls. The diffusion time of a molecule over a length L follows from random walk considerations as

$$t_{diff} = L^2/(\Lambda v) \qquad (17)$$

where Λ is the mean free path and v the molecular velocity. From this it follows that the time is proportional to pressure; it amounts for N_2 and CO to about 45 msec at 10 Torr for L=1 cm. If pure CO with a radiative lifetime of 30 msec is excited in the axial radiation beam about 1 cm from the walls of the experimental cell, 50% of the molecules arrive at the walls with their vibrational energy still intact. According to Table I, the maximum efficiency of cooling is displayed in Figure 3(a) as 0,0037. The heat signal given off for 50% of these molecules would result in a heat peak about 200 times larger than the cooling peak actually seen. In fact, any net heat produced would have to be less than 10% of the cooling peak before it disappears in the noise. This seems to indicate that the branching ratio for collisional energy conversion into heat of the gas is less than 0.1%. Similar conclusions can be reached by inspecting traces of gas mixtures at sufficiently low pressures [i.e., where (VRT) contributions are still excluded]. It is, of course, conceivable that the entire vibrational energy is absorbed as heat by the wall. This is an extremely unlikely process, since the molecule would still return into the gas with a substantial fraction of that energy. More likely is the alternative that the wall collisions are entirely elastic. Another possibility is quenching of the vibrational energy by photon emission. Further work is needed for a definite answer to these questions which are of potential practical interest.

6. PRACTICAL ASPECTS OF THE RESULTS FOR NASA RELATED INTERESTS

It is appropriate at this point to refer to the opening section of this report in which the motivation and expectations of this work have been discussed. The possibility of quasi-isentropic laser engine processes, operating with thermal cycles, has had few believers. In the main, doubts have centered on the feasibility of the required laser induced cooling cycles which had never been demonstrated. It is true that certain methods of reducing gas temperatures by coherent radiation had been shown to be valid. However, where the cooling was substantial, it affected only a relatively small number of molecules, and where the gas masses were macroscopic, the temperature reduction amounted to only a very small fraction of 1 K. In fact, none of these processes satisfied simultaneously the three cooling conditions postulated in Section 1.

6.1 Operational Requirements

The cooling effects demonstrated in this project originate in an irradiated gas column of about 10 mm^3. However, they were produced by a single laser pulse of about 2 mJ absorbed energy. These modest dimensions were limited by the scope of the project rather than by barriers of the present state of the art. CO_2 lasers with pulse repetition rates of more than 10^5 Hz have been built,[8] and pulse energies of second harmonic radiation from nonlinear crystals can be expected to reach larger values in the future.

Increase of the pump energy does not necessarily effect a corresponding increase in heat withdrawal. The CO molecules can be pumped only to equal populations in v=1 and v=0 at which point the gas is no longer absorbing (saturation). During a laser pulse duration of 10^{-7} sec. and at 10% CO concentration in 100 Torr N_2, each molecule per-

forms about 100 collisions, and practically in each of these rotational/translational energy is exchanged. Thus, the pulse time is amply sufficient to establish a thermal equilibrium of the rotational/translational states. On the other hand, a vibrationally excited CO molecule must make many collisions with N_2 molecules (perhaps as many as $2 \cdot 10^4$), before one of them transfers the vibrational energy from CO to N_2. Thus, mere increase of radiation intensity, after saturation is reached, does not increase cooling. If, however, the pulse time is spread over about 10 μsec, or the same energy is delivered in a sufficient number of weaker pulses, then there is sufficient time for the vibrational exchange. Thus, the upscaling of the cooling effects in CO/N_2 is contingent on the operation with a CO_2 laser either of a high pulse repetition rate, or of microsecond pulse times. From the measurements reported, it is clear that CO^*/CO^* interaction are not important at high dilution of CO by N_2. Nevertheless, the CO pressure should not be larger than required for sufficient absorption of the pump radiation so as to render the radiative time constant as large as possible. With these provisions, the process can withdraw much more heat per unit gas volume than in the very short pulses, approaching the theoretical value of $\Delta T = -120$ K for a single 10 μsec pulse (or an equivalent number of weaker pulses).

6.2 Outlook For Applications

Consideration of remotely operated quasi-isentropic laser engines are premature unless sufficient pump powers are available. However, resonance excitation of CO is possible with a variety of sources, and prospects for reaching significant powers are excellent. The mixture of CO/N_2 selected for these demonstration experiments is, of course, not necessarily the best choice for practical devices. Reference (2) lists other mixed gas combinations and also discusses various engine operating cycles. The underlying rule is that one has to separate the step of heat withdrawal (which compensates later heat rejection) from the step of vibrational heat release (which is used for conversion into work) either in time, in space, or both. The possibility of separa-

tion in time is in fact verified, at least in principle, by the traces obtained for CO/N_2 cooling and subsequent heating which may be 50-200 msec apart. In the experiment, the vibrational energy was released as spontaneous emission, whereas in an engine it is released by (VRT) processes during the compression step. Nevertheless, there is strong corroboration of the two-stroke piston engine concept in which the gas needs little thermal contact with the walls, one stroke occurring during cooling, the other serving heating.[2]

Applications closer at hand concern processes of cooling, and in particular, of isolated samples. It is anticipated from the measurement that at least 10% of the pump radiation power can be converted into heat withdrawn. An example is the use for detector cooling on satellites. A single radiation pulse may reduce the temperature by up to 120 K. Schemes of multistage cooling, either by molecular or mechanical means are projected to reduce the temperature to about 40 K. However, certain questions have yet to be answered for such schemes, requiring further work.

REFERENCES

1. (a) M. Garbuny, Laser Energy Conversion Symposium, K. W. Billman, ed., NASA-Ames, 18-19 January 1973; NASA TM X-62, 269; (b) M. Garbuny, Second Laser Energy Conversion Symposium, K. W. Billman, ed., NASA-Ames, 27-28 January 1975, NASA SP-395; (c) M. Garbuny and M. J. Pechersky, Final Report Contract NAS2-8372; (d) M. Garbuny and M. J. Pechersky, Appl. Opt. 15, 1141 (1976).

2. M. Garbuny, Final report on NAS2-9185; also, J. Chem. Phys., 67: 5676 (1977).

3. W. H. Christiansen and A. Hertzberg, Proc. IEEE 61, 1060 (1973); A. Hertzberg, Ref. 1 b, pp. 33-34.

4. M. Garbuny, Optics Comm. 18, 77 (1976).

5. G. Herzberg, "Spectra of Diatomic Molecules", Van Nostrand Reinhold Co. (1950).

6. N. Djeu Optics Comm. 26, 354 (1978).

7. M. Garbuny and T. Henningsen, Final Report, NASA-Ames Contract NAS2-10078, June 3, 1980.

8. N. Menyuk, G. W. Iseler, and A. Mooradian, Appl. Phys. Lett., 29, 422 (1976).

9. J. D. Feichtner and G. W. Roland, Appl. Optics 11, 993 (1972).

REPORT DISTRIBUTION

Recipient	Address
NASA Project Manager (17)	NASA-Lewis Research Center Attn: B. L. Sater (MS-77-4) 21000 Brookpark Road Cleveland, Ohio 44135
NASA-Lewis Contracting Officer (1)	NASA-Lewis Research Center Attn: D. F. Hoffman (MS-500-305) 21000 Brookpark Road Cleveland, Ohio 44135
Patent Counsel (1)	NASA-Lewis Research Center Attn: N. T. Musial (MS-500-318) 21000 Brookpark Road Cleveland, Ohio 44135
NASA Headquarters Technical Information Abstracting and Dissemination Facility (25)	NASA Scientific and Technical Information Facility Attn: Accessioning Department Post Office Box 8757 Baltimore/Washington Airport, Maryland 21240
Technical Liaison (1)	E. E. Bailey AFAPL/DO Wright Patterson Air Force Base, Ohio 45433
Lewis Library (2)	NASA-Lewis Research Center Attn: Library (MS-60-3) 21000 Brookpark Road Cleveland, Ohio 44135
Lewis Management Services Division (1)	NASA-Lewis Research Center Attn: Report Control Office (MS-60-1) 21000 Brookpark Road Cleveland, Ohio 44135
NASA Headquarters Space Power Systems (2)	NASA Headquarters (1) Attn: J. P. Mullin, RTS-6 (2) Attn: D. C. Byers, RTS-6 Washington, DC 20546